

# A Review of Concentric Annular Heat Pipes

A. NOURI-BORUJERDI and M. LAYEGHI

School of Mechanical Engineering, Sharif University of Technology, Tehran, Iran

*A detailed description of a concentric annular heat pipe (CAHP) operation is presented in low to moderate temperature ranges (50–200°C). The steady-state response of a CAHP to various heat fluxes in the evaporator and condenser sections are discussed. Two-dimensional mathematical modeling of the fluid flow and heat transfer in the annular vapor space and the wicks are described. The fundamental aspects and limitations of the operation of a CAHP are also discussed. Previously used numerical and experimental approaches for the analysis of the CAHPs and some related concepts are reviewed. The Navier-Stokes and similar equations are recommended for the simulation of fluid flow and heat transfer in the annular vapor space and the wicks. A number of important concepts, such as two-phase flow, heat transfer in the heat pipe wicks, the vapor–liquid interface conditions, design considerations, testing, and manufacture of a CAHP, are also briefly discussed. The results of this research have shown that the available numerical and experimental data in the literature are sufficiently accurate in many applications. However, new mathematical models and experimental works are needed for the better design and manufacture of various types of CAHPs.*

## INTRODUCTION

The concept of using heat pipe was originally initiated by King and Perkins in their patents registered in the mid-1800s [1, 2]. These patents describe a device referred to as the *Perkins tube*, which utilizes either single or two-phase processes to transfer heat from a furnace to a boiler. Gay [3] obtained a patent on a device similar to the Perkins tube in which a number of vertical tubes were arranged with the evaporator located below the condenser. These devices, which are actually classified as *thermosyphons*, laid the groundwork for the later development of what is now commonly referred to as a heat pipe. The heat pipe concept received relatively little attention, however, until Grover et al. [4] published the results of an independent investigation and applied the term “heat pipe” for the first time. Since that time, heat pipes have been employed in various applications.

A conventional heat pipe, which operates on a closed two-phase cycle, consists of a sealed container lined with a wicking material. The container of the heat pipe can be constructed from metals, ceramics, composite materials, or glass. In all applications, careful consideration must be given to the material type,

thermophysical properties, and compatibility. For example, the container material must be compatible with both the working fluid and the wicking material, strong enough to withstand pressures associated with the saturation temperatures encountered during heat addition and normal operation, and have a high thermal conductivity. In addition to these characteristics, which are primarily concerned with the internal effects, the container material must often be resistant to corrosion resulting from interaction with the environment and malleable enough to be formed into the appropriate size and shape.

To operate the heat pipe, the container is evacuated and back-filled with just enough liquid to fully saturate the wicks. Because only pure liquid and vapor are present within the container, the working fluid will remain at saturation conditions as long as the operating temperature is between the triple point and the critical state. The selection of a suitable fluid with appropriate thermophysical properties has an important role in the design and manufacture of heat pipes. The operating temperature range must be adequate for each specific application. In addition, consideration must be given to the ability of the working fluid wettability and to the wick and wall materials. The working fluid can vary from nitrogen or helium for very low-temperature (cryogenic) heat pipes to lithium, potassium, or sodium for very high-temperature (liquid metal) heat pipes. Further criteria for the selection of the working fluids have been presented by Faghri [5], Dunn and Reay [6], and Heine and Groll [7], in which a number of other

Address correspondence to Dr. A. Nouri-Borujerdi, School of Mechanical Engineering, Sharif University of Technology, P.O. Box 11365-9567, Azadi Ave., Tehran, Iran. E-mail: anoui@sharif.edu

factors including the liquid and vapor pressure, flow limits, and compatibility of the materials are considered.

The wicking material can be made up of screens, wire meshes, sintered metal powders, woven fiberglass, or grooves. The wicking material usually has two functions in heat pipe operation: it returns the working fluid from the condenser to the evaporator and ensures that the working fluid is evenly distributed over the evaporator surface. Gaugler [8] utilized a wicking material as part of a passive two-phase heat transfer device capable of transferring large quantities of heat with a minimal temperature drop. Trefethen [9] reexamined this concept in connection with the space program and in the form of a patent application [10].

A heat pipe consists of three distinct sections: an evaporator or heat addition section, a condenser or heat rejection section, and an adiabatic or isothermal section. These three parts have equal importance and can significantly affect the performance of a heat pipe. When heat is added to the evaporator section of the container, the working fluid present in the wicking structure is heated until it vaporizes. The high temperature and corresponding high pressure in the evaporator section cause the vapor to flow to the cooler condenser section, where the vapor condenses and releases its latent heat of vaporization. The capillary forces existing in the wicking structure then pump the liquid back to the evaporator. The evaporator and condenser sections of a heat pipe function independently, needing only common liquid and vapor streams. For this reason, the area over which heat is introduced can differ in size and shape from the area over which it is rejected, provided that the rate at which the liquid is vaporized does not exceed the rate at which it can be condensed. Hence, high heat fluxes generated over relatively small areas can be dissipated over larger areas with reduced heat fluxes. This is particularly useful in the thermal control of electronic components and systems, because it allows the high heat fluxes generated at the component level to be reduced and free or forced convection to be used to dissipate the heat.

Because heat pipes operate on a closed two-phase cycle, the heat transfer capacity may be several orders of magnitude greater than even the best solid conductors. This results in a relatively small thermal resistance and allows the physical separation of the evaporator and condenser without a high penalty in overall temperature drop. Also, any increase in the heat flux in the evaporator may result in an increase in the rate at which the working fluid is vaporized without a significant increase in the operating temperature. Thus, the heat pipe can function as a nearly isothermal device, adjusting the evaporation rate to accommodate a wide range of power inputs while maintaining a relatively constant temperature. Another advantage of a heat pipe is its small thermal response time. Because heat pipes utilize a closed two-phase cycle, the thermal response time is considerably less than for other types of heat transfer devices, particularly solid conductors. This response time is not a function of length.

The heat pipe application includes temperature and humidity control, cooling large diesel pistons [11], the removal of heat from laser diodes and other small localized heat-generating devices, the removal of heat dissipation from the leading edge of

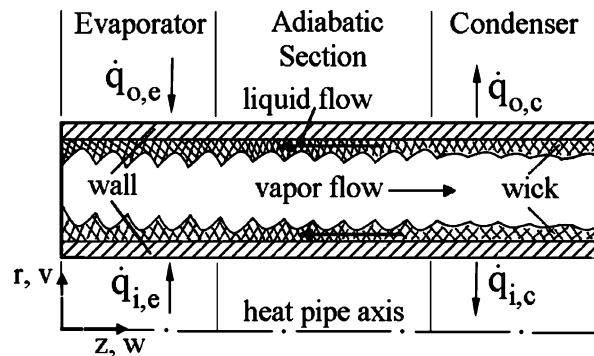


Figure 1 Schematic of a CAHP and coordinate system.

hypersonic aircraft, and numerous other industrial applications in a wide range of temperatures. Finally, the high heat transfer characteristic, the ability to maintain constant evaporator temperatures under different heat flux levels, and the diversity and variability of evaporator and condenser sizes make heat pipes effective devices for use in many diverse situations.

A concentric annular heat pipe (CAHP) is similar to the conventional heat pipe except that the cross-section of the vapor space is annular instead of circular (see Figure 1). This enables the designer to place the wick materials on the inside of the outer pipe and the outside of the inner pipe. In this manner, the surface area for heat addition and rejection can be increased significantly without increasing the outer diameter of the heat pipe. The sizes and shapes of CAHPs are almost as varied as the applications. Vapor- and liquid-flow cross-sectional areas also vary significantly, from those encountered in rectangular cross-section annular heat pipes, which have very large flow areas, to very small micro annular heat pipes. The dry-out phenomenon, which is a serious limitation in a conventional heat pipe, can be effectively controlled by using a CAHP at a specific heat flux. The properly designed CAHP can have a very long life and its use in space applications and online thermal controls is actual, reliable, and highly recommended. Finally, the use of the CAHPs can be twice as effective as conventional heat pipes in compact heat exchanger applications.

The CAHP applications are also similar to the conventional heat pipes; however, the use of the CAHPs in some applications is preferred. These applications include the cooling of annular spaces (such as transformers or capacitors) in electrical components and the annular cooling of heat sinks cores. In addition, the annular heat pipe has been used as an isothermal furnace with excellent results due to its temperature flattening capabilities and fast response time to a cold charge [5]. It is also well suited for use in reduced gravity environments. CAHP can be fixed or variable in length and either rigid or flexible for situations where relative motion or vibration poses a problem.

Traditionally, the analysis of the performance of a heat pipe consists of the analysis of vapor flow, the liquid flow through the wick, and the vapor-liquid interface. The last two parts of this analysis are basically similar for different heat pipe structures. For non-conventional heat pipes, however, the dynamics of

vapor flow is more complex due to the geometry and boundary specifications. Mathematical modeling of a heat pipe involves a variety of subjects, such as heat and fluid flow in porous media, two-phase flow, heat and mass transfer, and fluid dynamics. Fortunately, a number of simple models have shown good agreement with the experimental results and been used extensively in the literature. In many cases, the available two-dimensional models have shown to be accurate and reliable. Many investigators have analyzed the conventional heat pipes using a variety of numerical and experimental techniques. Faghri [5], Dunn and Reay [6], Chi [12], Terpstra and Van Veen [13], and Peterson [14] have published several of these techniques, theories, and applications of different heat pipe structures. There are, however, only a limited number of works concerning the CAHP in the literature.

Recently, Nouri-Borujerdi and Layeghi [15] simulated the vapor flow and pressure drop along a CAHP for various symmetric and asymmetric heat addition and rejection circumstances. They showed that under asymmetric heat addition and rejection circumstances, a number of recirculation zones may be created at both the evaporator and condenser sections. They discussed qualitatively that these recirculation zones can be very effective zones for increasing heat transfer between objects of different diameters even at high radial Reynolds numbers.

In this paper, an overview of theoretical and experimental results for the analysis of low-temperature conventional and concentric annular heat pipes is presented. The main objective is to review the previous experiences and models that have been used or can be used for the analysis of low-temperature CAHPs. For vapor flow analysis, the elliptic, parabolic, and incompressible models are described, and some important conclusions are drawn. The governing equations of vapor flow and liquid flow in the wicks and vapor–liquid interfaces and appropriate boundary conditions for vapor flow analysis are discussed. The CAHP limitations and advantages are also discussed, and useful methods for better design and manufacture of a CAHP are recommended.

### LIQUID FLOW THROUGH WICK AND CAPILLARY PRESSURE

A capillary pressure exists at the vapor–liquid interface due to the surface tension of the working fluid and the curved structure of the interface (see Figure 1). The difference in the curvature of the menisci along the vapor–liquid interface causes the capillary pressure to change along the pipe. This capillary pressure gradient circulates the fluid against the liquid and vapor pressure losses and adverse body forces such as gravity. The capillary pressure created by the menisci in the wick pumps the condensed fluid back to the evaporator section. Therefore, the heat pipe can continuously transport the latent heat of vaporization from the evaporator to the condenser section. This process will continue as long as there is a sufficient capillary pressure to drive the condensate back to the evaporator. The menisci at the vapor–liquid interface are highly curved in the evaporator section due to the

fact that the liquid recedes into the pores of the wick. During the condensation process, the menisci in the condenser section are nearly flat.

In their experimental study of a CAHP, Faghri and Thomas [16] found that not all of the working fluid that condenses onto the inner pipe wall in the condenser section reaches the inner evaporator section. A meniscus was formed in the condenser section where the inner pipe and the end cap were joined, which allowed part of the working fluid that condensed onto the inner pipe to be drained down to the outer pipe. They described that this phenomenon is the result of communication of the working fluid between the inner and outer pipes. This phenomenon should be prevented by proper wick and end cap design, which would increase the amount of heat that can be transferred by the inner pipe.

### VAPOR FLOW IN THE ANNULAR SPACE

The vapor pressure changes along the concentric heat pipe are due to friction, inertia, and evaporation and condensation effects, while the liquid pressure in the wick changes mainly as a result of friction. Figure 2 shows a typical axial variation of the liquid and vapor pressures for low vapor flow rates. The pressure distribution along the inner and outer wicks is also nearly similar. Thus, only one pressure distribution is shown. The maximum local capillary pressure should be equal to the sum of the pressure drops in the vapor and the liquid across each of the heat pipe wicks in the absence of body forces. When body forces such as adverse gravitational forces are present, the liquid pressure drop is greater, indicating that the capillary pressure must be higher in order to return the liquid to the evaporator for a given heat input.

At moderate vapor flow rates, dynamic effects cause vapor pressure drop and recovery along the condenser section. The local vapor–liquid pressure difference is small, but this pressure gradient approaches zero at the condenser end cap similar to the low vapor flow rate case. Again, the capillary pressure difference at the evaporator end cap should be balanced by the sum of the total pressure drop in the vapor and liquid across the heat pipe.

The general trend at high vapor flow rates with low liquid pressure drops is different from the above two cases. The vapor pressure drop can exceed the liquid pressure drop in the

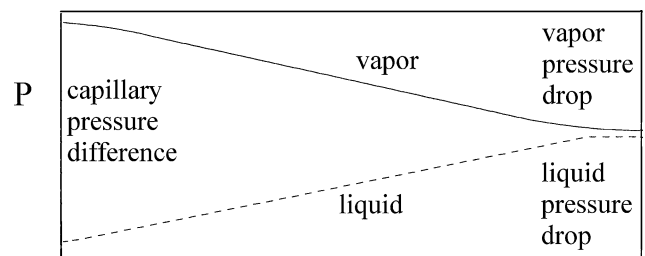


Figure 2 Vapor and liquid pressure distributions in a CAHP.

condenser section. In such a case, the liquid pressure would be higher than the vapor pressure in the condenser section if the pressure in the liquid and vapor phases are equal at the condenser end cap. In reality, the wet point is not situated at the condenser end cap, and the menisci at the vapor–liquid interface in the condenser are curved.

It is also important to note that the above description for the physics of the operation of a CAHP is restricted to a nearly symmetric heat addition and rejection condition. The symmetric heat addition and rejection conditions are conditions such that all radial Reynolds numbers in the evaporator and condenser sections are the same. In some special situations, called *asymmetric conditions*, this assumption may not be valid. Under the asymmetric heat addition and rejection conditions, the vapor–liquid interface behavior and heat transfer through heat pipe, walls, wicks, and vapor can be more complex, and various asymmetric phenomena may be observed and need to be more studied.

### LIMITATIONS ON THE HEAT TRANSPORT CAPACITY

There are a number of parameters that put limitations on the steady-state operation of a CAHP. Each parameter usually corresponds to a physical phenomenon that can have a substantial effect on the heat transport capacity of a CAHP. Although the heat pipe performance and operation are strongly dependent on the shape, the working fluid, and the wick structure, the fundamental phenomenon that governs the operation arises from the difference in the capillary pressure across the vapor–liquid interfaces in the evaporator and condenser sections. When this capillary pressure is not sufficient to promote the flow of liquid from the condenser to the evaporator, the heat pipe is said to have reached its capillary limit, and dry-out of the evaporator wick occurs. For a CAHP, the dry-out phenomenon can occur for both the inner and the outer pipe wicks in the evaporator section. Thus, the capillary limit can be defined as a condition in which the dry-out phenomenon occurs at least in one of the CAHP wicks, and the maximum capillary limit is the maximum amount of heat addition in which dry-out phenomenon occurs in both wicks.

The capillary limit is approximately determined using a simple one-dimensional analysis of the vapor and liquid flows in a CAHP with symmetric heat addition and rejection as follows:

$$\begin{aligned}
 (\dot{q}_e)_{\max} &= \frac{2\pi \left[ \sigma \left( \frac{\cos\theta_i}{r_{c,i}} + \frac{\cos\theta_o}{r_{c,o}} \right) - (\rho_l - \rho_v)gL \sin\alpha \right] h_{fg}}{\left[ \frac{\mu_v f_v \text{Re}_{v,z}}{\rho_v (R_{vo}^2 - R_{vi}^2)(R_{vo} - R_{vi})^2} + \frac{q^* \mu_l}{K_i \rho_l (R_{vi}^2 - R_{li}^2)} + \frac{(1-q^*)\mu_l}{K_o \rho_l (R_{lo}^2 - R_{vo}^2)} \right] L_{\text{eff}}}
 \end{aligned} \quad (1)$$

where

$$q^* = \dot{q}_{i,e} / \dot{q}_e = \dot{q}_{i,c} / \dot{q}_c$$

and

$$\dot{q}_e = \dot{q}_c = \dot{q}_{i,e} + \dot{q}_{o,e}.$$

It has been shown that Eq. (1) has good accuracy in the range of low to moderate radial Reynolds numbers. In derivation of Eq. (1), it has been assumed that the wet and dry points are located at both ends of the heat pipe. However, this assumption may not be valid in a number of situations. The dry point is a point at the vapor–liquid interface where the meniscus has a minimum radius of curvature and usually occurs in the evaporator at the point furthest from the condenser region. The wet point is a point where the vapor pressure and liquid pressure are approximately equal or where the radius of curvature approaches infinity, and it is usually located at the condenser section.

Faghri and Thomas [16] showed experimentally that the maximum stable operating limit of a CAHP can be 82 percent more than a conventional heat pipe with the same outer diameter. During steady-state operation, several other important mechanisms can limit the maximum amount of heat that a CAHP can transfer. Among these are the viscous limit, sonic limit, entrainment limit, and boiling limit. The capillary wicking limit and viscous limit deal with the pressure drops occurring in the liquid and vapor phases, respectively. The sonic limit results from the occurrence of choked flow in the annular vapor space, while the entrainment limit is due to the high vapor–liquid shear forces developed as the vapor passes in a counter-flow direction over the liquid-saturated wicks. Faghri [5] has also analyzed the sonic limit of a CAHP. Prediction of the entrainment limit in a CAHP can be more complex especially when the heat pipe operation is under the asymmetric heat addition and rejection condition. All of the above limits are axial heat flux limits; that is, they are a function of the axial heat transport capacity of the heat pipe. The boiling limit, however, is a radial heat flux limit and is reached when the heat flux applied in the evaporation portion is so high that nucleate boiling occurs in each of the evaporator wicks. This creates vapor bubbles that partially block the return of fluid and may ultimately lead to premature dry-out of the evaporator.

For low- to moderate-temperature annular heat pipes, the most significant of these limits is the capillary wicking limit. However, the significance of this limit decreases somewhat for reduced gravity applications. In very low-temperature applications, such as those using cryogenic working fluids, either the viscous limit or capillary limit occurs first, while in high-temperature heat pipes, such as those that use liquid metal working fluids, the sonic and entrainment limits are of increased importance.

The theory and fundamental phenomenon that cause each of those limitations have been the subject of a considerable number of investigations for conventional heat pipes. The most famous works have been presented and discussed by Dunn and Reay [6], Brennan and Kroliczek [10], Chi [12], Cotter [17], Chisholm [18], Tien [19], Feldman [20]. However, there are numerous published papers during the past forty years—but only

a limited number of publications about the operation limitations in a CAHP [21].

The appropriate boundary conditions are

$$w_v(0, r) = v_v(0, r) = 0, \tag{6a}$$

$$w_v(L, r) = v_v(L, r) = 0, \tag{6b}$$

$$w_v(z, R_i) = w_v(z, R_o) = 0 \tag{6c}$$

**MATHEMATICAL MODELLING**

Mathematical modeling of a CAHP can be categorized in three sections: vapor flow model, liquid flow through wicks, and vapor-liquid interface analysis. There are a number of models that can be used in each category, but here the most important and applicable models are discussed. The basis of the models is on their validity and extensive use for the analysis of conventional heat pipes and CAHPs. However, the validity and reliability of some of these models must be checked numerically or experimentally for each special application.

$$v_v(z, R_j) = \begin{cases} \pm V_{j,e} & 0 < z < L_e \\ 0 & L_e < z < L_e + L_a \\ \mp V_{j,c} & L_e + L_a < z < L \end{cases} \tag{6d}$$

$$P_v(0, R_i < r < R_o) = 0 \tag{6e}$$

The uniform radial blowing and suction velocities at the inner and outer walls in the evaporator and condenser are computed as (see Figure 1).

$$V_{j,e} = \frac{\dot{q}_{j,e}}{2\pi R_j L_e \rho_v h_{fg}} \tag{7a}$$

$$V_{j,c} = \frac{\dot{q}_{j,c}}{2\pi R_j L_c \rho_v h_{fg}} \tag{7b}$$

**VAPOR FLOW MODELS**

**Elliptic Model**

The evaporation and condensation are modeled as a uniform injection and suction, but no phase change is actually involved in the calculations [22]. The energy equation is usually solved numerically only for the vapor region. The elliptic Navier-Stokes and energy equations associated with this axisymmetric problem are considered, and both evaporation and condensation are considered to occur at the surface of the heat pipe walls and assumed to be uniform. This model has been used by Faghri [21] for the vapor flow analysis of a CAHP. The conservation of mass, momentum, and energy equations for the incompressible vapor flow analysis are as follows (see Figure 1):

where

$$j = i, o,$$

indicating the location at the inner or outer wall. The  $\pm$  signs refer to the direction of the radial velocity,  $e$  and  $c$  refer to the evaporator and condenser, and  $\dot{q}_{j,e}$  and  $\dot{q}_{j,c}$  are the heat transfer to the evaporator and from the condenser sections, respectively. The temperature at the vapor-liquid interface of the evaporator and condenser is calculated approximately using Clausius-Clapeyron equation

$$T_{int} = \frac{1}{\frac{1}{T_{sat}} - \frac{R}{h_{fg}} \ln \frac{P_v}{P_{sat}}} \tag{8}$$

where  $P_{sat}$  and  $T_{sat}$  are saturated pressure and temperature as a reference state and  $R$  is the vapor gas constant.

$$\frac{w_v}{z} + \frac{1}{r} \frac{r}{r} (r v_v) = 0 \tag{2}$$

$$\rho_v \left[ w_v \frac{w_v}{z} + v_v \frac{w_v}{r} \right] = -\frac{P_v}{z} + \mu_v \left[ \frac{1}{r} \frac{r}{r} \left( r \frac{w_v}{r} \right) + \frac{^2 w_v}{z^2} \right] \tag{3}$$

$$\rho_v \left[ w_v \frac{v_v}{z} + v_v \frac{v_v}{r} \right] = -\frac{P_v}{r} + \mu_v \left[ \frac{1}{r} \frac{r}{r} \left( r \frac{v_v}{r} \right) - \frac{v_v}{r^2} + \frac{^2 v_v}{z^2} \right] \tag{4}$$

$$\rho_v C_{p_v} \left[ w_v \frac{T_v}{z} + v_v \frac{T_v}{r} \right] = k_v \left[ \frac{1}{r} \frac{r}{r} \left( r \frac{T_v}{r} \right) + \frac{^2 T_v}{z^2} \right] \tag{5}$$

**Parabolic Model**

In this model, the parabolized version of the Navier-Stokes equations can be derived from Eqs. (3, 4) by neglecting the terms  $\frac{\phi^2}{z^2}$  for  $\phi = w_v, v_v$  and  $T_v$ . Faghri [23] used this model for analyzing the two-dimensional, steady, and incompressible flow of vapor in a CAHP. The results have shown good agreement with elliptic model too, but in the condenser section, the elliptic model seems to be more accurate. This is because the physics of the vapor motion in the condenser section is clearly of the elliptic type. The results have shown that the flow reverses in long condenser segments or at very high condensation rates, and the parabolic presentation provides a sufficiently accurate picture of the vapor pressure variation at both low and high evaporation and condensation rates.

**Fully Developed Model**

From the study by Faghri and Parvani [22], one can generalize that the vapor flow in an annular heat pipe becomes fully developed in a very short distance from the evaporator end cap. This profile repeats itself in the adiabatic and condenser sections for low as well as moderate radial Reynolds numbers. The entry distance is not of significance in many practical applications. The criterion for a fully developed flow is that the normalized axial vapor velocity is invariant along the pipe. A very interesting feature of the numerical results given by Faghri and Parvani [22] was that the vapor axial velocity was similar for various radial Reynolds numbers, including the case with zero inner and outer radial Reynolds numbers. The fully developed normalized velocity profile for annular flow for zero blowing velocity can be easily obtained analytically as:

$$w_v = 2\bar{w}_a \frac{2[1 - r^{*2} - \frac{1-R_i^{*2}}{\ln R_i^*} \ln r^*]}{\frac{1-R_i^{*4}}{1-R_i^{*2}} + \frac{1-R_o^{*2}}{\ln R_i^*}} \quad (9)$$

where

$$r^* = r/R_o$$

$$R_i^* = R_i/R_o$$

and  $\bar{w}_a$  is the mean axial vapor velocity in the adiabatic section:

$$\bar{w}_a = \frac{\dot{q}_{i,e} + \dot{q}_{o,e}}{\rho_v \pi (R_o^2 - R_i^2) h_{fg}} \quad (10)$$

Faghri and Parvani [22] used Eqs. (2–4) with appropriate boundary conditions for the analysis of the evaporator, condenser and adiabatic sections of a CAHP. They derived a number of analytical expressions for determining the pressure drop along various parts of a CAHP. It has been found that the fully developed results predict the pressure variation when the flow reverses as well.

In Figure 3, the results of the various vapor flow models are compared. The agreement between the fully developed solution and complete solution of the two-dimensional elliptic version of the conservation equations indicates that the axial velocity profile becomes fully developed in a short distance and stays parabolic all along the length of the heat pipe for both cases. Figures 3a and 3b show that flow reversal in the condenser did not occur for the low and moderate radial Reynolds number cases because the condenser zone is short. There is a region where the flow reverses in the condenser for high radial Reynolds numbers, which is shown by the large pressure recovery in the condenser in Figure 3c.

Typical velocity vectors and streamlines in a CAHP when flow reversal occurs in the condenser section are shown in Figure 4. These results have been obtained by solving Eqs. (2–5) numerically using a finite volume method based on staggered

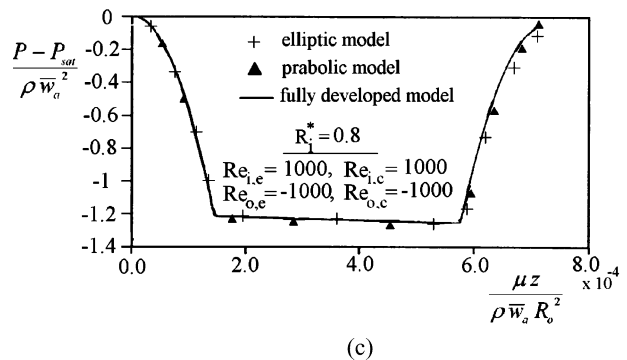
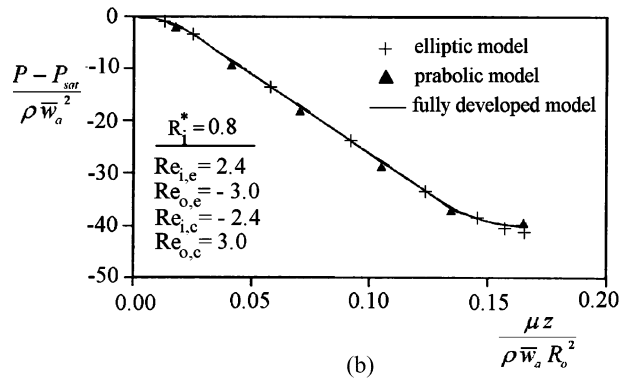
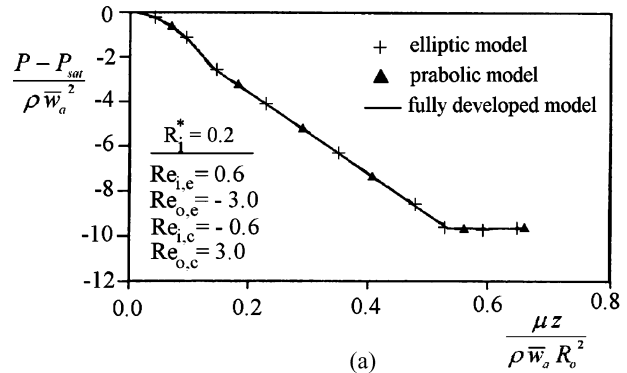


**Figure 3** Pressure distribution of the vapor for three vapor flow models for different Reynolds numbers, (a) Low, (b) Moderate, and (c) Large, Faghri [5].

grids [24]. A uniform  $200 \times 40$  mesh has been used in this numerical analysis.

**LIQUID FLOW THROUGH A WICK**

In the analysis of the liquid flow in the wick structures, it is generally assumed that the liquid flow is a steady, two-dimensional, incompressible laminar flow with negligible body forces. The fluid and the wick structure are assumed to be in local thermal equilibrium, and the velocities in the radial and axial directions are the local volume-averaged velocities over a cross-section of the wick region instead of the absolute velocities. Also, the inner and outer wall wicks are assumed to

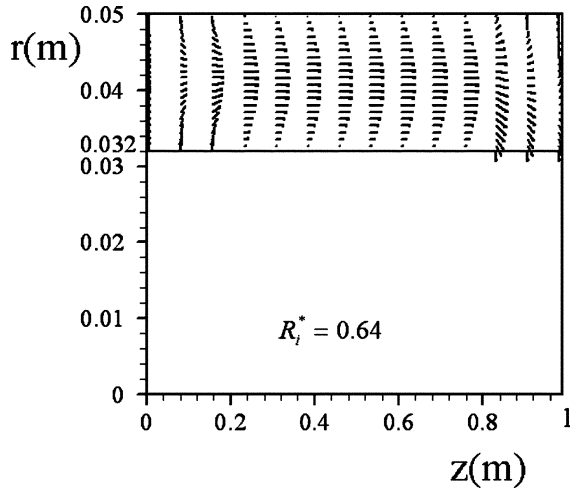


Figure 4 Velocity vectors in a CAHP for  $Re_r = 100$ .

be isotropic, homogeneous, and the same type. The steady-state conservation equations for mass and momentum in the wick regions can be written as:

$$\frac{w}{z} + \frac{1}{r} \frac{d}{dr}(rv) = 0 \tag{11}$$

$$\frac{\rho}{2} \left( v \frac{w}{r} + w \frac{w}{z} \right) = -\frac{p}{z} - \frac{\mu w}{K} + \mu \left[ \frac{1}{r} \frac{d}{dr} \left( r \frac{w}{r} \right) + \frac{2w}{z^2} \right] \tag{12}$$

$$\frac{\rho}{2} \left( v \frac{v}{r} + w \frac{v}{z} \right) = -\frac{p}{r} - \frac{\mu v}{K} + \mu \left[ \frac{1}{r} \frac{d}{dr} \left( r \frac{v}{r} \right) - \frac{v}{r^2} + \frac{2v}{z^2} \right] \tag{13}$$

$$\rho C_p \left( v \frac{T}{r} + w \frac{T}{z} \right) = \frac{1}{r} \frac{d}{dr} \left( r k_{eff} \frac{T}{r} \right) + \frac{1}{z} \left[ k_{eff} \frac{2T}{z^2} \right] \tag{14}$$

The boundary conditions are

$$w(0, r) = v(0, r) = w(L, r) = v(L, r) = 0,$$

$$\begin{cases} R_{li} < r < R_{vi}, & \text{if } j = i \\ R_{vo} < r < R_{lo} & \text{if } j = o \end{cases} \tag{15}$$

$$w(z, R_{lj}) = v(z, R_{lj}) = w(z, R_{vj}) = 0, \quad j = i, o \tag{16}$$

where

$$v_j(z, R_{vj}) = \begin{cases} \pm \frac{\rho_v}{\rho} V_{j,e} & 0 < z < L_e \\ 0 & L_e < z < L_e + L_a, \quad j = i, o \\ \mp \frac{\rho_v}{\rho} V_{j,c} & L_e + L_a \leq z < L_t \end{cases} \tag{17}$$

Indexes  $j = i, o$  indicate the inner and outer wall wicks, respectively. The  $\pm$  signs indicate the direction of the injection or suction mean vapor velocity at the vapor–liquid interface,  $\rho$  is the porosity of the liquid, and  $\mu$  is the viscosity. Also,  $w$  and  $v$  are the axial and radial volume-averaged velocities at the wall wicks, respectively;  $K$  is the permeability of the porous material, that characterizes its ability to transmit liquid under the action of an applied pressure gradient; and  $V_{j,e}$  and  $V_{j,c}$  are calculated using Eqs. (7a, b). The effective thermal conductivity of the wick is dependent on both the wick material and the working fluid. The effective thermal conductivity for various types of wick structures have been presented by Faghri [5].

**VAPOR-LIQUID INTERFACE ANALYSIS**

Proper analysis of vapor–liquid interfaces in an operational heat pipe has an important role in predicting the real heat pipe limitations. The work of Beavers and Josef [25] was one of the first attempts to study the fluid flow boundary conditions at the interface region. They performed experiments and detected a slip in the velocity at the interface.

Neale and Nader [26] presented one of the earlier attempts regarding this type of boundary condition. In this study, the authors proposed continuity in both the velocity and the velocity gradient at the interface by introducing the Brinkman term in the momentum equation for the porous side. Vafai and Thiyagaraja [27] analytically studied the fluid flow and heat transfer for three types of interfaces—namely, the interface between two different porous media, the interface separating a porous medium from a fluid region, and the interface between a porous medium and an impermeable medium. Continuity of shear stress and heat flux were taken into account in their study while employing the Forchheimer-Extended Darcy equation in their analysis. Vafai and Kim [28] presented an exact solution for the fluid flow at the interface between a porous medium and a fluid layer, including the inertia and boundary effects. In this study, the shear stress in the fluid and the porous medium were taken to be equal at the interface region. Other studies consider the same set of boundary conditions for the fluid flow and heat transfer used in the works presented by Vafai and Thiyagaraja [27], Poulikakos and Kazmierczak [29], Vafai and Kim [30], Kim and Choi [31], and Ochoa-Tapia and Whitaker [32].

Sahraoui and Kaviany [33] have proposed a hybrid interface condition for the heat transfer part. They used the continuity of

the heat flux at the interface along with a slip in the temperature at the interface. Ochoa-Tapia and Whitaker [34, 35] have proposed a hybrid interface condition in which a jump in the shear stress at the interface region is assumed. In their study, the shear stress jump is inversely proportional to the permeability of the porous medium. This proposed set of interface conditions was used in the works presented by Kuznetsov [36–40]. Ochoa-Tapia and Whitaker [41] have presented another shear stress jump boundary condition where the inertia effects become important. Further same investigation by Ochoa-Tapia and Whitaker [42] has presented another hybrid interface condition for the heat transfer part in which they introduce a jump condition to account for a possible excess in the heat flux at the interface. Alazmi and Vafai [43] presented a comprehensive analysis of variants within the transport models in porous media. In their study, four major categories—namely, constant porosity, variable porosity, thermal dispersion, and local thermal non-equilibrium—were considered in great detail. More recently, Alazmi and Vafai [44] critically examined the differences in the fluid flow and heat transfer characteristics due to different interface conditions, including all of the aforementioned models. They performed a systematic analysis of the variances among different boundary conditions, showing that in general, the variances have a more pronounced effect on the velocity field, a substantially smaller effect on the temperature field, and an even smaller effect on the Nusselt number distributions.

The most important limitation that is directly related to the vapor–liquid interface is the entrainment limitation. The phenomenon of entrainment occurs when high velocity vapor flow pass over the vapor–liquid interface and entrain the small liquid drops from that interface. Many researchers have studied the entrainment limit in conventional heat pipes (e.g., [45, 46]), but the phenomenon of entrainment seems to be more complex, and the previous theoretical and experimental results are limited to a number of configurations, wick structures, and materials. The results of the previous works include a number of correlations, criteria, and simulations. The most accurate experimental result corresponds to an attractive approach followed by Kim and Peterson [46]. They review the twelve important models and completed extensive experiments with a copper–water, rectangular cross-section, 2.16 meters-long heat pipe. They also performed parametric studies and used computer modeling to compare their results. They classified the entrainment in their heat pipe experiment into three major modes: wave-induced, pulsating, and intermediate modes, according to not only the flow visualization experiment but also the temperature fluctuation patterns at the onset of the individual entrainment modes. Finally, they proposed a correlation for predicting the critical Weber number for the stability of the liquid interface. The other important result of the experiments done by Kim and Peterson [46] was that the capillary limit occurred before boiling or entrainment limit.

It can be found from the previous research that for the analysis of the vapor–liquid interface in a CAHP, both experimental and numerical analysis are required. On the other hand, some of the

results of the previous studies related to conventional heat pipe can be used or generalized for the concentric annular case. It seems to be useful to evaluate the vapor–liquid interface behavior in a long CAHP by creating a visible region at the adiabatic section and utilizing advanced measurement systems. The experimental results can then be used to validate the numerical results.

## TEST PROCEDURES

Once the heat pipe is fully instrumented, setup in the rig (see Figure 5), the condenser jacket flow may be started and heat can be applied to the evaporator section. Heat input should preferably be applied at first in steps, building up to design capability and allowing the temperatures along the heat pipe to achieve a steady-state before adding more power. When the steady-state condition is reached, power input, power output, and the temperature profile along the heat pipe should be noted [47]. If temperature profiles change uniformly with adding more power, the heat pipe is operating satisfactorily. However, several modes of failure can occur, all being recognizable by temperature changes at the evaporator or condenser section.

The most common failure is dry-out created by excessive power input at the evaporator section. It is characterized by a rapid rise in evaporator temperature compared to other regions of the heat pipe. Once dry-out has occurred, the wick has to be reprimed, and this is best achieved by cutting off the power input completely. When the temperature difference along the heat pipe drops to 1–2°C, the power may be reapplied. The second failure mechanism recognizable by an increased evaporator temperature and known as overheating occurs at elevated temperatures. In general, the evaporator temperature does not increase as quickly as in a burn-out condition, but these two phenomena are difficult to distinguish.

Temperature changes at the condenser section can also point to failure mechanisms or a decrease in performance. A sudden drop in temperature at the end of the heat pipe downstream of the cooling jacket occurring at high powers can be attributed to the collection of working fluid in that region, insulating the wall and creating a cold spot. This has been called cool-out. Complete failure need not necessarily occur when this happens, but the overall temperature difference will be substantially increased, and the effective heat pipe length is reduced. A similar drop in

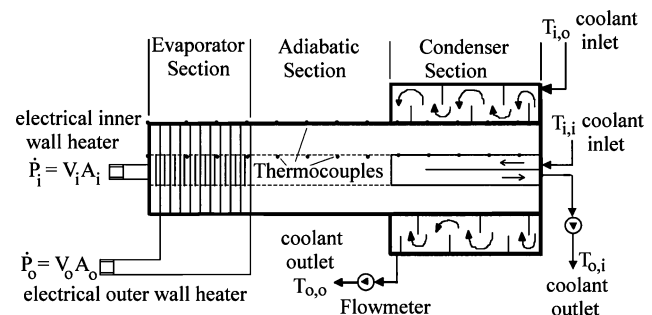


Figure 5 Schematic of a CAHP with heating and cooling systems.



temperature can occur when the fluid inventory is greater than that needed to completely saturate the wick. The vapor tends to push the excess fluid to the cooler end of the heat pipe, where because of the small vapor space volume, a small excess of fluid will create a long cold region.

### ***Container Materials***

Of the many materials available for the container, three are by far the most common in use—name copper, aluminum, and stainless steel. Copper is eminently satisfactory for heat pipes operating between 0–200°C in applications such as electronics cooling. While commercially pure copper tube is suitable, the oxygen-free high conductivity type is preferable. Like aluminum and stainless steel, the material is readily available and can be obtained in a wide variety of diameters and wall thicknesses in its tubular form.

### ***Wick Structure***

A very large number of wick structures can be used in various types of CAHPs. The most common form of wick is a woven wire mesh or twill, which can be made in many metals. In this case, the spot welding is a convenient technique for preserving or attaching the wick to the wall in cases where the heat pipe diameter is sufficiently large to permit insertion of an electrode. Failing this, a coil spring can be used. It is very important to make a close contact between the wicks and heat pipe walls. Diffusion bonding is a useful process that can be used to ensure such a close contact.

A similar structure having intimate contact with the heat pipe wall is a sintered wick. This process involves bonding together a large number of particles in the form of a packed metal powder. The pore size of the wick thus formed can be arranged to suit by selecting powders having a particular size. This kind of wick structure is described in Dunn and Reay [6]. The sintered wicks are extensively used nowadays because they can be manufactured with high conductivity property and can return the working fluid effectively even when the heat pipe is tilted. Other wick structures, such as vapor deposition manufactured wicks, grooved wicks, felts, and foams, can also be used as a wick structure in a CAHP.

### ***Cleaning of Container and Wick***

All of the materials used in a heat pipe must be clean. Cleanliness achieves two objectives: it ensures that the working fluid will wet the materials and that no foreign matter is present that could hinder capillary action or create incompatibilities. Cleanliness is difficult to quantify, and the best test is to add a drop of demineralized water to the cleaned surface. If the drop immediately spreads across the surface or is completely absorbed into

the wick, good wetting has occurred, and satisfactory cleanliness has been achieved. If the working fluid is a solvent, such as acetone, no extreme precautions are necessary to ensure good wetting, and an acid pickle followed by a rinse in the working fluid appears to be satisfactory. Pickling of copper demands a 50/50 phosphoric acid and nitric acid solution. An ultrasonic cleaning bath is a useful addition for speeding up the cleaning process but is by no means essential for low-temperature heat pipes.

### ***Material Outgassing***

When the wick or wall material is under a vacuum, gases will be drawn out, particularly if the components are metallic. If not removed prior to sealing of the heat pipe, these gases could collect in the heat pipe vapor space. The process is known as out gassing. Out gassing does not appear to be a problem in low-temperature heat pipes. Generally, the out gassing rate is strongly dependent on temperature, increasing rapidly as the component temperature is raised.

### ***Fitting of Wicks and End Caps***

The fitting of wicks depends on the type of the wicks and the geometry of the heat pipe. For conventional heat pipes, the fitting process of mesh wicks is readily done by coiling a spring tightly around a mandrel, giving a good internal clearance in the heat pipe. However, for CAHPs, an annular mandrel can be used to fit the mesh wicks. An annular mandrel can also be used for the installation of sintered wicks.

The fitting of end caps is normally carried out by argon arc welding. This need not be done in a glove box and is applicable to copper, stainless steel, and aluminum heat pipes. The advantage of welding over brazing or soldering is that no flux is required; therefore, the inside of cleaned pipes do not suffer from possible contamination. The use of a thermal absorbent paste to surround the area of heat pipe local to the weld can considerably reduce the amount of oxide formed. Electron beam welding may also be used for heat pipe assembly, but this added expense cannot be justified in most applications.

### ***Leak Detection***

All welds on heat pipes should be checked for leaks. If quality control is to be maintained, a rigorous leak check procedure is necessary. The best way to test the heat pipe for leaks is to use a mass spectrometer, which can be used to evaluate the heat pipe to a very high vacuum, better than  $10^{-5}$  Torr, using a diffusion pump. The weld area is then tested by directing a small jet of helium gas onto it. If a leak is present, the gauge head on the mass spectrometer will sense the presence of helium once it enters the heat pipe. After an investigation of the weld areas and

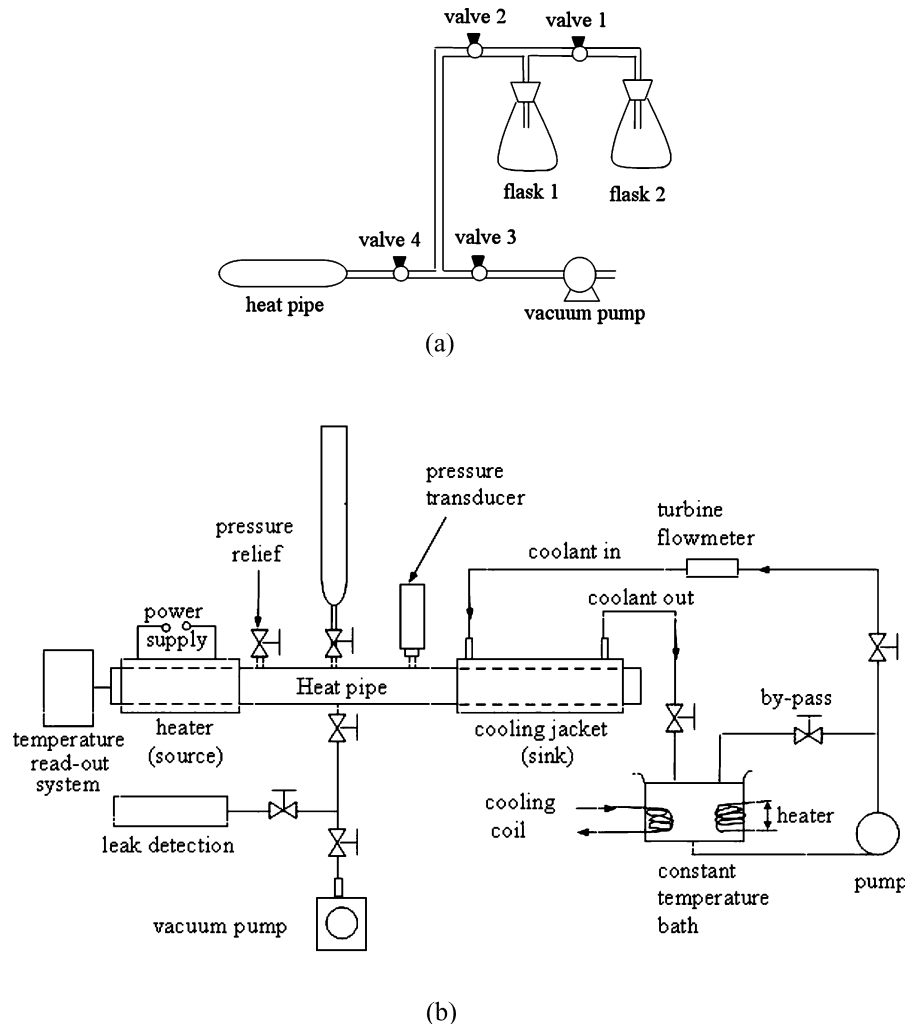


Figure 6 Schematic of two different typical filling rigs for low-temperature CAHP.

location of the general leak area(s), if present, a hypodermic needle can be attached to the helium line and careful traversing of the suspected region can lead to very accurate identification of the leak position, possibly necessitating only a very local rewelding procedure to seal it.

### Preparation of the Working Fluid

The working fluid should be the most highly pure fluid available, and further purification may be necessary following purchase. This may be carried out by distillation. Low-temperature working fluids, such as acetone, methanol, and ammonia, in the presence of water can lead to incompatibilities, and the minimum possible water content should be achieved. A procedure recommended for all heat pipe working fluids used up to 200°C is freeze-degassing. This process removes all dissolved gases from the working fluid—if the gases are not removed, they could be released during heat pipe operation and collected in the condenser section. Freeze-degassing may be carried out on the heat

pipe filling rig described in Figure 6 and is a simple process. The fluid is placed in a container in the rig directly connected to the vacuum system and is frozen by surrounding the container with a flask containing liquid nitrogen. When the working fluid is completely frozen, the container is evacuated and released and the liquid nitrogen flask removed. The working fluid is then allowed to thaw, and dissolved gases will be seen to bubble out of the liquid. The working fluid is then refrozen and the process repeated. All gases will be removed after three or four freezing cycles. The liquid will now be in a sufficiently pure state for insertion into the heat pipe.

### Filling Rig

The usual method for filling a heat pipe with a working fluid is constructing an appropriate filling rig, as shown in Figure 6a [14]. The rig may also be used to carry out the processes such as working fluid degassing, working fluid metering, heat pipe degassing, and heat pipe filling with inert gas (Figure 6b) [48].

The material of construction for pipe-work is generally either glass or stainless steel. Glass has advantages when handling liquids in that the presence of liquid droplets in the duct-work can be observed and their vaporization under vacuum noted. Stainless steel has obvious strength benefits and must be used for all high-temperature work, together with high-temperature packless valves such as Hoke-Bellows valves. The rig that is shown in Figure 6 is for low-temperature heat pipe manufacture.

Valves used in vacuum rigs should preferably have 'O' ring seals, and it is important to ensure that the ductwork is not too long or has a small diameter, as this can greatly increase evacuation times. The vacuum pump may be the diffusion type or absorption pump containing a molecular sieve, which produces vacuums as low as  $10^{-4}$  Torr. It is, of course, advisable to refer to experts in the field of high vacuum technology when considering designing a filling rig.

### **Sealing**

Unless the heat pipe is to be used as a demonstration unit or for life testing, in which case a valve may be retained on one end, the filling tube must be permanently sealed. With copper, this is conveniently carried out using a tool that will crimp and cold weld the filling tube. If stainless steel or aluminum is used as the heat pipe filling tube material, crimping followed by argon arc welding is a more satisfactory technique. After sealing, the filling tube may be protected by a cap having an outer diameter the same as that of the heat pipe wall. The cap may be filled with solder, a metal-loaded resin, or any other suitable material.

### **Network Model**

Zuo and Faghri [49] performed a network thermodynamic analysis of the conventional heat pipe. They provided a unique view into the physics behind the heat pipe operation, which was considered a thermal network of various components. Thermal heat pipe behavior was described by first order, linear, ordinary differential equations. They assumed that the working fluid undergoes a thermodynamic cycle and analyzed the cycle by T-s diagrams. They analyzed both transient and steady-state operation of the conventional heat pipe. They found that successful establishment of the thermodynamic cycle requires compatibility between the thermophysical properties of the working fluid envelop material combination and geometric dimensions of the heat pipe. If this requirement is not satisfied, the heat pipe cannot function properly. Their analysis provided a reasonably accurate and particularly simple way to transient heat pipe analysis and design. A similar procedure can be followed for transient analysis of a CAHP.

### **Entropy Generation in a Heat Pipe System**

Khalkhali et al. [50] developed a thermodynamic model of a conventional cylindrical heat pipe based on the second law of

thermodynamics. They performed a detailed parametric analysis in which the effects of various heat pipe parameters on entropy generation were examined. They concluded that there exists a thermodynamic requirement that the vapor temperature must be greater than a certain value in order for the heat pipe to operate. There is also an optimum condenser ambient temperature that corresponds to a minimum entropy generation. It is also found that both the condenser ambient temperature and the convection heat transfer coefficient in the transport section must be correspondingly adjusted to obtain a minimum entropy generation. To reduce the entropy generation in fluid flow, the evaporator length should be as small as possible and the wick cross-sectional hydraulic diameter as large as possible. Temperature drop in the vapor flow increases the entropy generation and correspondingly decreases the second law efficiency. Thus, an optimum heat pipe should be based on the minimization of the entropy generation, which ensures a minimum loss in availability in the system. A similar procedure can be followed for the analysis of entropy generation in a CAHP system.

### **Vapor-Liquid Coupling and Non-Darcian Transport**

Zhu and Vafai [51] presented a two-dimensional analytical model for low-temperature cylindrical heat pipes. They obtained a closed form solution that incorporated vapor-liquid interfacial hydrodynamic coupling and non-Darcian transport through the porous wick for the first time for predicting the vapor and liquid velocity and pressure distributions. The effects of the vapor-liquid interfacial hydro-dynamic coupling and non-Darcian transport through the porous wick on the vapor and liquid velocity and pressure distributions as well as the heat pipe capillary limit have been discussed and assessed. The presented closed-form analytical solutions provided a quick, accurate prediction method for low-temperature heat pipe operation and were found to be in very good agreement with both experimental and numerical results. The results also show that the interfacial effects are small and can be neglected. However substantial errors can occur when using Darcy's law in calculating the liquid pressure distributions as well as the maximum heat removal capability of the heat pipe. Khrustalev and Faghri [52] have done an important analysis of the coupling between the liquid and vapor flow in miniature passages. Zhang and Wang [53] have done the most recent thermodynamic analysis of the vapor-liquid interface. For a CAHP, a two-dimensional analysis similar to that used by Zhu and Vafai [51] can be developed. This is the subject of the authors' current research.

### **Making Improvement in Performance of a Heat Pipe**

Joudi and Wiwit [54] experimentally investigated the performance of gravity-assisted wickless heat pipes and modified heat pipes with a separator in the adiabatic section. They found that the presence of the adiabatic separator caused a marked

improvement (maximum 35%) in all heat pipes tested for all lengths and inclination angles. A number of similar techniques can be used to improve the CAHP performance, effectively.

## CONCLUSIONS

Concentric annular heat pipe (CAHP) is an effective device in various heat transfer, heat recovery, and heat exchanger applications. It can be designed and manufactured in a wide range of sizes and shapes and can have a wide temperature range of operation. It can be utilized in spacecraft applications, large industrial applications, or as a heat sink to cool electronic components and packages. CAHP can also be used to connect two conventional heat pipes side-by-side to transfer the heat to a place far from the heat source or device. The use of micro CAHPs is particularly promising, as increases in power density will require the use of phase change heat transfer for temperature control. Many types of CAHPs can be used as a low weight, long-life solution to various types of thermal problems. Although investigations continue to determine and evaluate new wick materials, working fluids, and efficient sizes and configurations, little additional research is needed on the more simple devices provided that materials with proven compatibility are chosen and that proper cleaning, filling, and sealing procedures are followed.

The fluid flow and heat transfer in a CAHP can be accurately simulated using the presented elliptic models. Vapor flow analysis in a CAHP can be done using an elliptic or parabolic version of Navier-Stokes equations and fully developed solutions. The results are very close to each other, and the difference between the various vapor flow models is negligible at least for low to moderate radial Reynolds numbers. It also has been found that the models work well for the prediction of vapor flow reversal. However, transition to turbulence phenomenon was not considered in the previous research, and further studies and more complete models are needed to predict the flow reversal and transition to turbulence phenomena for a real condition in a CAHP. The model can be used to analyze the steady-state vapor flow and heat transfer in a CAHP. A two-dimensional model for analyzing the liquid flow through wicks has also been presented. It is found that the vapor-liquid interface models in the previous research have many simplifications. But the errors corresponding to these simplifications have been negligible, at least for the cases studied by Faghri [5] and Alazmi and Vafai [44]. But, by implementing further details such as the effects of the vapor shear stress on the vapor-liquid interface in the mathematical models, it is possible to get a better physical insight into the various phenomena that affect the performance of the CAHP. The effects of the various parameters such as liquid fill ratio, non-condensable gases, and property variations can be considered in the future studies. The phenomenon of transition to turbulence in a CAHP is also an attractive concept for both numerical and experimental studies.

Limitations on the heat transport capacity of a low-temperature CAHP are very similar to those for a conventional heat

pipe. The most important one is the capillary limit. During steady-state operation, several other important mechanisms can limit the maximum amount of heat that a CAHP can transfer. Among these are the viscous limit, sonic limit, entrainment limit, and boiling limit. However, exact mathematical modeling and prediction of these limitations needs to be more studied for a particular CAHP.

A network model of the cylindrical heat pipe, consisting of a network of thermal resistance and a working fluid cycle, can be first developed to analyze the heat pipe transients. Then the steady-state working fluid circulation and the related thermodynamic constraints can be analyzed by thermodynamic T-s diagrams. Entropy generation and the effects of vapor-liquid coupling and non-Darcian transport of liquid in the wicks in a conventional heat pipe or CAHP are interesting and important concepts that can be studied in the future.

Making improvements in performance of a CAHP is possible at least by adding a separator in the adiabatic section. However, some other innovations seem to be applicable, especially using new numerical techniques and experimental tools.

## NOMENCLATURE

$A$	ampere
$C_p$	heat capacity at constant pressure
$f$	friction factor
$g$	acceleration of gravity
$h_{fg}$	latent heat of vaporization
$k$	thermal conductivity
$K$	permeability
$L$	length
$P$	pressure
$\dot{P}$	power
$\dot{q}$	heat transfer rate
$r$	radial coordinate
$R$	gas constant, radius
Re	radial Reynolds number, $\rho RV/\mu$
$T$	temperature
$v$	radial velocity
$V$	radial blowing and suction velocity or volt
$w$	axial velocity
$z$	axial coordinate

## Greek Symbols

$\alpha$	tilt angle
	porosity
$\theta$	contact angle
$\mu$	viscosity
$\rho$	density
$\sigma$	surface tension
$\phi$	general variable

**Subscripts**

<i>a</i>	adiabatic
<i>c</i>	condenser, capillary
<i>e</i>	evaporator
<i>eff</i>	effective
<i>i</i>	inner, inlet
<i>int</i>	interface
<i>l</i>	liquid
<i>max</i>	maximum
<i>o</i>	outer, outlet
<i>sat</i>	saturation
<i>v</i>	vapor

**Superscripts**

—	average
*	dimensionless, $( )^* = ( )/R_o$

**REFERENCES**

- [1] King, C. R., Perkins Hermetic Tube Boilers, *The Engineer*, vol. 152, pp. 405–406, 1931.
- [2] Perkins, L. P., and Buck, W. E., Improvements in Devices for the Diffusion or Transference of Heat, UK Patent 22,272, London, England, 1892.
- [3] Gay, F. W., Heat Transfer Means, U.S. Patent 1,725,906, 1929.
- [4] Grover, G. M., Cotter, T. P., and Erikson, G. F., Structures of Very High Thermal Conductivity, *Journal of Applied Physics*, vol. 35, pp. 1190–1191, 1964.
- [5] Faghri, A., *Heat Pipe Science and Technology*, Taylor & Francis, Washington, DC, 1995.
- [6] Dunn, P. D., and Reay, D. A., *Heat Pipes*, Pergamon, Oxford, 1982.
- [7] Heine, D., and Groll, M., Compatibility of Organic Fluids with Commercial Structure Materials for Use in Heat Pipes, *Proc. 5th International Heat Pipe Conference*, Tsukuba, Japan, pp. 170–174, 1984.
- [8] Gaugler, R. S., Heat Transfer Devices, U.S. Patent 2,350,348, 1944.
- [9] Trefethen, L., On the Surface Tension Pumping of Liquids or a Possible Role of the Candlewick in Space Exploration, *G. E. Tech. Info.*, serial no. 615 D114, Detroit, MI, 1962.
- [10] Brennan, P. J., and Kroliczek, E. J., *Heat Pipe Design Handbook*, B&K Engineering, Towson, MD, 1979.
- [11] Wang, Q., Cao, Y., Wang, R., Mignano, F., and Chen, G., Studies of a Heat Pipe Cooled Piston Crown, *ASME Journal of Engineering for Turbines and Power*, vol. 122, pp. 99–105, 2000.
- [12] Chi, S. W., *Heat Pipe Theory and Practice*, Hemisphere, Washington, DC, 1976.
- [13] Terpstra, M., and Van Veen, J. G., *Heat Pipes: Construction and Application*, Elsevier Applied Science, New York, 1987.
- [14] Peterson, G. P., *An Introduction to Heat Pipes: Modeling, Testing, and Applications*, John Wiley, New York, 1994.
- [15] Nouri-Borujerdi, A., and Layeghi, M., A Numerical Analysis of Vapor Flow in Concentric Annular Heat Pipes, *ASME Journal of Fluids Engineering*, vol. 126, pp. 442–448, 2004.
- [16] Faghri, A., and Thomas S., Performance Characteristics of a Concentric Annular Heat Pipe, Part I: Experimental Prediction and Analysis of the Capillary Limit, *Journal of Heat Transfer*, vol. 111, pp. 851–857, 1989.
- [17] Cotter, T. P., Theory of Heat Pipes, Los Alamos National Laboratory Report no. LA-3246-MS, The University of California, Los Alamos, NM, 1964.
- [18] Chisholm, D., *The Heat Pipe*, Mills and Boon, London, England, 1971.
- [19] Tien, C. L., Fluid Mechanics of Heat Pipes, *Annual Review of Fluid Mechanics*, vol. 2, pp. 167–186, 1975.
- [20] Feldman, K. T., *The Heat Pipe: Theory, Design and Applications*, Technology Application Center, University of New Mexico, Albuquerque, NM, 1976.
- [21] Faghri, A., Performance Characteristics of a Concentric Annular Heat Pipe Part II: Vapor Flow Analysis, *Journal of Heat Transfer*, vol. 111, pp. 851–857, 1989.
- [22] Faghri, A., and Parvani, S., Numerical Analysis of Laminar Flow in a Double-Walled Annular Heat Pipe, *Journal of Thermophysics and Heat Transfer*, vol. 2, no. 2, pp. 165–171, 1988.
- [23] Faghri, A., Vapor Flow Analysis in a Double-Walled Concentric Heat Pipe, *Numerical Heat Transfer*, vol. 10, no. 6, pp. 583–595, 1986.
- [24] Ferziger, J. H., and Perić, M., *Computational Methods for Fluid Dynamics*, 2nd ed., Springer-Verlag, Berlin, Heidelberg, 1999.
- [25] Beavers, G., and Josef, D. D., Boundary Conditions at a Naturally Permeable Wall, *Journal of Fluid Mechanics*, vol. 30, pp. 197–207, 1967.
- [26] Neale, G., and Nader, W., Practical Significance of Brinkman's Extension of Darcy's Law: Coupled Parallel Flows within a Channel and a Bonding Porous Medium, *Can. J. Chem. Engrg.*, vol. 52, pp. 475–478, 1974.
- [27] Vafai, K., and Thiyagaraja, R., Analysis of Flow and Heat Transfer at the Interface Region of a Porous Medium, *International Journal of Heat Mass Transfer*, vol. 30, pp. 1391–1405, 1987.
- [28] Vafai, K., and Kim, S. J., Fluid Mechanics of the Interface Region Between a Porous Medium and a Fluid Layer—An Exact Solution, *International Journal of Heat Fluid Flow*, vol. 11, pp. 254–256, 1990.
- [29] Poulikakos, D., and Kazmierczak, M., Forced Convection in a Duct Partially Filled with a Porous Material, *Journal of Heat Transfer*, vol. 109, pp. 653–662, 1987.
- [30] Vafai, K., and Kim, S. J., Analysis of Surface Enhancement by a Porous Substrate, *Journal of Heat Transfer*, vol. 112, pp. 700–706, 1990.
- [31] Kim, S. J., and Choi, C. Y., Convection Heat Transfer in Porous and Overlying Layers Heated from Below, *International Journal of Heat Mass Transfer*, vol. 39, pp. 319–329, 1996.
- [32] Ochoa-Tapia, J. A., and Whitaker, S., Heat Transfer at the Boundary between a Porous Medium and a Homogeneous Fluid, *International Journal of Heat Mass Transfer*, vol. 40, pp. 2691–2707, 1997.
- [33] Sahraoui, M., and Kaviany, M., Slip and No Slip Temperature Boundary Conditions at the Interface of Porous, Plain Media:

- Convection, *International Journal of Heat Mass Transfer*, vol. 37, pp. 1029–1044, 1997.
- [34] Ochoa-Tapia, J. A., and Whitaker, S., Momentum Transfer at the Boundary between a Porous Medium and a Homogeneous Fluid I: Theoretical Development, *International Journal of Heat Mass Transfer*, vol. 38, pp. 2635–2646, 1995.
- [35] Ochoa-Tapia, J. A., and Whitaker, S., Momentum Transfer at the Boundary between a Porous Medium and a Homogeneous Fluid II: Comparison with Experiment, *International Journal of Heat Mass Transfer*, vol. 38, pp. 2647–2655, 1995.
- [36] Kuznetsov, A. V., Analytical Investigation of the Fluid Flow in the Interface Region between a Porous Medium and a Clear Fluid in Channels Partially Filled with a Porous Medium, *Applied Scientific Research*, vol. 56, pp. 53–67, 1996.
- [37] Kuznetsov, A. V., Influence of the Stress Jump Condition at the Porous-Medium/Clear-Fluid Interface on a Flow at a Porous Wall, *International Communications Heat Mass Transfer*, vol. 24, pp. 401–410, 1997.
- [38] Kuznetsov, A. V., Analytical Investigation of Coette Flow in a Composite Channel Partially Filled with a Porous Medium and Partially Filled with a Clear Fluid, *International Journal of Heat Mass Transfer*, vol. 41, pp. 2556–2560, 1998.
- [39] Kuznetsov, A. V., Analytical Study of Fluid Flow and Heat Transfer during Forced Convection in a Composite Channel Partially Filled with a Brinkman-Forchheimer Porous Medium Flow, *Turbulence Combustion*, vol. 60, pp. 173–192, 1998.
- [40] Kuznetsov, A. V., Fluid Mechanics and Heat Transfer in the Interface Region between a Porous Medium and a Fluid Layer: A Boundary Layer Solution, *Journal of Porous Media*, vol. 2, no. 3, pp. 309–321, 1999.
- [41] Ochoa-Tapia, J. A., and Whitaker, S., Momentum Jump Condition at the Boundary between a Porous Medium and a Homogeneous Fluid: Inertial Effects, *Journal of Porous Media*, vol. 1, pp. 201–217, 1998.
- [42] Ochoa-Tapia, J. A., and Whitaker, S., Heat Transfer at the Boundary between a Porous Medium and a Homogeneous Fluid: The One-Equation Model, *Journal of Porous Media*, vol. 1, pp. 31–46, 1998.
- [43] Alazmi, B., and Vafai, K., Analysis of Variants within the Porous Media Transport Models, *Journal of Heat Transfer*, vol. 122, pp. 303–326, 2000.
- [44] Alazmi, B., and Vafai, K., Analysis of Fluid Flow and Heat Transfer Interfacial Conditions between a Porous Medium and a Fluid Layer, *International Journal of Heat Mass Transfer*, vol. 44, pp. 1735–1749, 2001.
- [45] Tien, C. L., and Chung, K. S., Entrainment Limits in Heat Pipes, *AIAA Journal*, vol. 17, no. 6, pp. 643–646, 1979.
- [46] Kim, B. H., and Peterson, G. P., Analysis of the Critical Weber Number at the Onset of Liquid Entrainment in Capillary-Driven Heat Pipes, *International Journal of Heat Mass Transfer*, vol. 38, no. 8, pp. 1427–1442, 1995.
- [47] Faghri, A., Performance Characteristics of an Annular Heat Pipe, in *Experiments in Heat Transfer and Thermodynamics*, ed. R. A. Granger, Cambridge University Press, London, 1994.
- [48] Colwell, G.T., and Chang, W.S., Measurements of the Transient Behavior of a Capillary Structure under Heavy Thermal Loading, *International Journal Heat Mass Transfer*, vol. 27, no. 4, pp. 541–551, 1984.
- [49] Zuo, Z. J., and Faghri, A., A Network Thermodynamic Analysis of the Heat Pipe, *International Journal of Heat Mass Transfer*, vol. 41, no. 11, pp. 1473–1484, 1998.
- [50] Khalkhali, H., Faghri, A., and Zuo, Z. J., Entropy Generation in a Heat Pipe System, *Applied Thermal Engineering*, vol. 19, pp. 1027–1043, 1999.
- [51] Zhu, N., and Vafai, K., Analysis of Cylindrical Heat Pipes Incorporating the Effects of Liquid–Vapor Coupling and Non-Darcian Transport—A Closed Form Solution, *International Journal of Heat Mass Transfer*, vol. 42, pp. 3405–3418, 1999.
- [52] Khrustalev, D., and Faghri, A., Coupled Liquid and Vapor Flow in Miniature Passages with Micro Grooves, *ASME Journal of Heat Transfer*, vol. 121, pp. 729–733, 1999.
- [53] Zhang, J. T., and Wang, B. X., Effect of Capillarity at Vapor–Liquid Interface on Phase Change without Surfactant, *International Journal of Heat Mass Transfer*, vol. 45, pp. 2689–2694, 2002.
- [54] Joudi, K. A., and Wiwit A. M., Improvements of Gravity-Assisted Wickless Heat Pipes, *Energy Conversion & Management*, vol. 41, pp. 2041–2061, 2000.



**Ali Nouri-Borujerdi** is a professor of Mechanical Engineering at Sharif University of Technology in Tehran, Iran. He received his Ph.D. degree from the University of Wisconsin at Madison, and he joined Sharif University of Technology in 1966. He has authored or co-authored more than forty publications in the field of heat transfer, computational fluid dynamics, porous media, and two-phase flow, including boiling and condensation, and acts as consultant to various industries.



**Mohammed Layeghi** is a Ph.D. student in the division of Thermal/ Fluid Sciences of Mechanical Engineering Department at Sharif University of Technology, Tehran, Iran. He received his Master's degree from Iran University of Science and Technology in 1998 and his B.Sc degree from Sharif University of Technology in 1996. His research interest is in the analysis and simulation of concentric annular heat pipes.